Supporting information

Synergy of Morphology and Phosphorization for Enhanced Peroxymonosulfate Activation over Magnetic Fe_3O_4 Catalysts

Haidong Lu [a], Congming Tang[a*], Kai Ma[b] and Xinli Li[a1*]

([a]School of Chemistry and Chemical Engineering, Chongqing University of Technology, Chongqing 400054, PR China; [b]Synthetic Lubricants Research Institute of Sinopec Lubricant Co., Ltd., Chongqing 400039, PR China)

S1. Preparation of catalysts

S1.1. RC-Fe_2O_3, THB-Fe_2O_3 and QC-Fe_2O_3

RC-Fe_2O_3: Under alkaline conditions, RC-Fe_2O_3 was synthesized by hydrothermal method and then calcined in air. In a typical experiment, 10 mmol of Fe $(NO_3)_3 \cdot 9H_2O$ and 36 mmol of urea $(CO(NH_2)_2)$ were dissolved in 60 mL of deionized water and stirred at room temperature for 30 minutes. Next, the obtained solution transferred to a 100 mL stainless steel hydrothermal reactor with the lined polytetrafluoroethylene, placed it in an oven, and maintained it at 120 ℃ for 8 hours. Then a precipitate was formed, washed several times with deionized water and anhydrous ethanol, and dried at 50 ℃ for 3 hours. The obtained sample was calcined in air at 500 ℃ for 3 hours.

THB-Fe_2O_3: 0.337g of $K_4[Fe(CN)_6] \cdot 3H_2O$ was dissolved in 40 mL of sodium carboxymethyl cellulose (CMC, 300-800 MPa s, 1.25 g L^{-1}) solution. Then, 0.5 g of polyvinylpyrrolidone (PVP-k30) and 0.30 mL of hydrazine hydrate solution ($N_2H_4 \cdot H_2O$, 80%) were added, and dispersed with ultrasonic treatment until PVP-k30 was completely dissolved. The mixture was trasferred to a 100 mL stainless steel hydrothermal reactor with the lined polytetrafluoroethylene, heated to 160 ℃, and remained at this temperature for 6 hours. After the hydrothermal reaction, the suspension was centrifuged, and the solid was washed four times with deionized water and once with ethanol. The

*Corresponding author. Tel.: +86 23 62563250, E-mail address: tcmtang2001@cqut.edu.cn (C. M. Tang) and lixinlitcm@163.com (X. L. Li).

sample was dried at 80 ° C for 5 hours and calcined in air at 300 ° C for 3 hours. The obtained sample was labeled as THB-Fe_2O_3.

QC-Fe_2O_3: The amounts of $K_4[Fe(CN)_6]\cdot 3H_2O$ and hydrazine hydrate solution were changed to 0.253 g and 0.90 mL, respectively. The other procedures were the same as those of THB- Fe_2O_3, and the obtained sample was marked as QC- Fe_2O_3.

S1.2. RC-Fe_3O_4, QC-Fe_3O_4 and THB-Fe_3O_4

RC-Fe_3O_4, QC-Fe_3O_4 and THB-Fe_3O_4 were prepared with lactic acid selective reduction. RC-Fe_3O_4: 0.5 g of RC-Fe_2O_3 was placed in tubular quartz reactor with an inner diameter of 4 mm, and both ends were sealed with quartz wool to fix sample. The sample was pretreated with high purity N_2 (flow rate 2.5 mL/min) at 360^{o}C for 1 h, and then lactic acid (10 wt%) was pumped into the quartz tubular reactor via a peristaltic pump with a flow rate of 2 mL/h, treated for 6 h, and the obtained sample was marked as RC-Fe_3O_4. QC-Fe_3O_4 and THB-Fe_3O_4 were prepared with the similar method, as long as the percussor of RC-Fe_2O_3 was changed to QC-Fe_2O_3 and THB-Fe_2O_3, respectively.

S1.3. P-RC-Fe_3O_4, P-QC-Fe_3O_4 and P-THB-Fe_3O_4

0.2 g of as-prepared RC-Fe_3O_4 was placed downstream and 2 g of sodium hypophosphite monohydrate placed upstream of a quartz boat in a tube furnace, heated to 400 ℃ at 5 ℃/min, and remained at 400 ℃ for 2 hours under a nitrogen atmosphere. The resultant sample was marked as P-RC-Fe_3O_4. QC-Fe_3O_4 and THB-Fe_3O_4 were treated with the similar method, respectively, and the obtained samples were marked as P-QC-Fe_3O_4 and P-THB-Fe_3O_4.

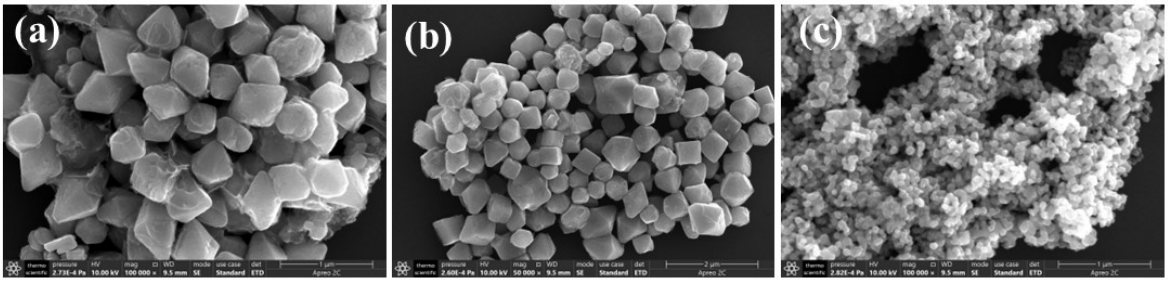

Fig. S1. Morphologies of nano-Fe_3O_4: (a) THB, (b) QC and (c) RC.

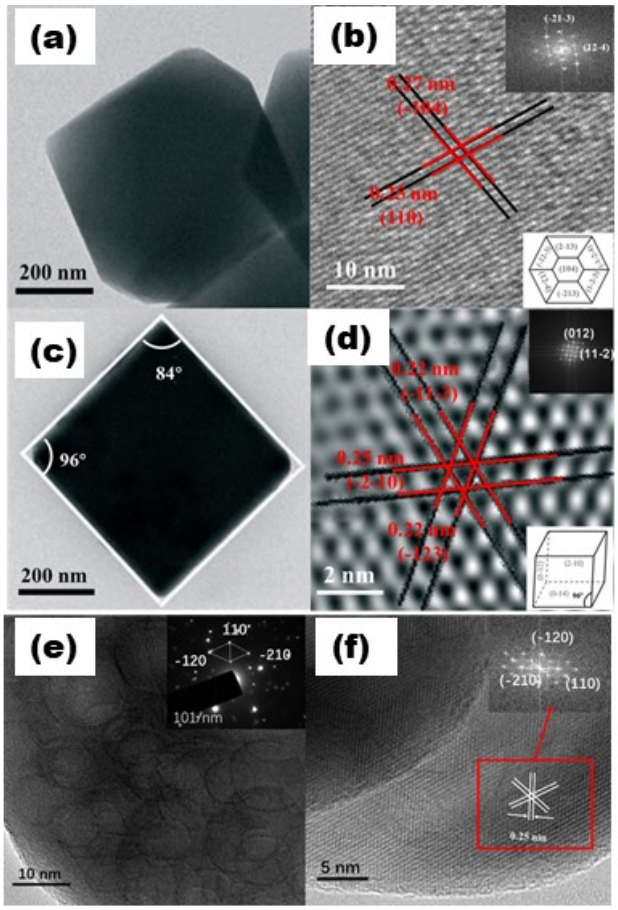

Fig. S2. Morphologies and structures of a-Fe_2O_3[1-2]. (a) TEM and (b) HRTEM images of a-Fe_2O_3-THB, insets: FFT pattern and drawing of a hexagon; (c) TEM and (d) HRTEM images of a-Fe_2O_3-QC, insets: FFT pattern and drawing of a cube; (e) TEM and (f) HRTEM images of the α-Fe_2O_3-RC, insets: SEAD pattern and FFT pattern.

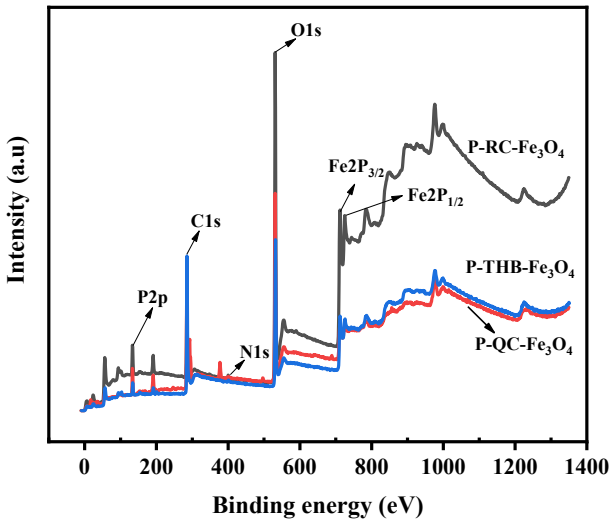

Fig. S3. XPS survey spectra of P-THB-Fe_3O_4, P-QC-Fe_3O_4 and P-RC-Fe_3O_4.

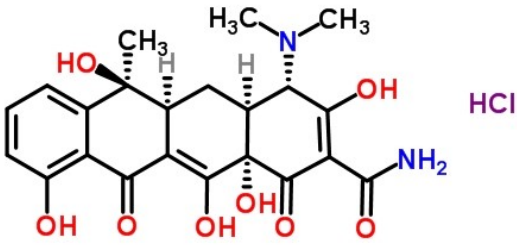

Fig. S4. Chemical structure of tetracycline (TC)

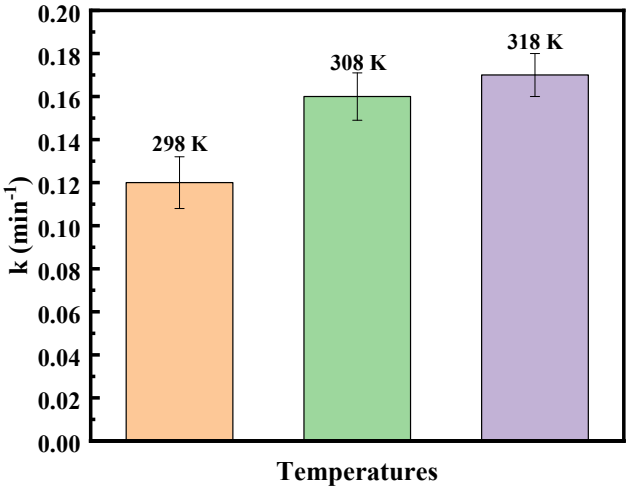

Fig. S5. Comparison of reaction rate constant of P-RC-Fe_3O_4/PMS system at different reaction temperatures

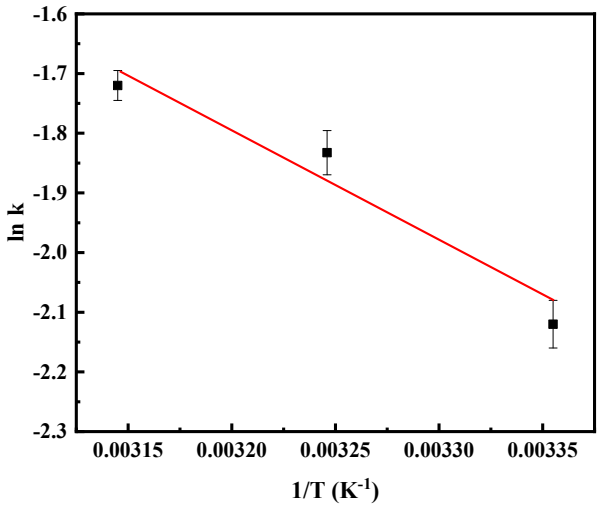

Fig. S6. Arrhenius plot of TC degradation over P-RC-Fe_3O_4/PMS system

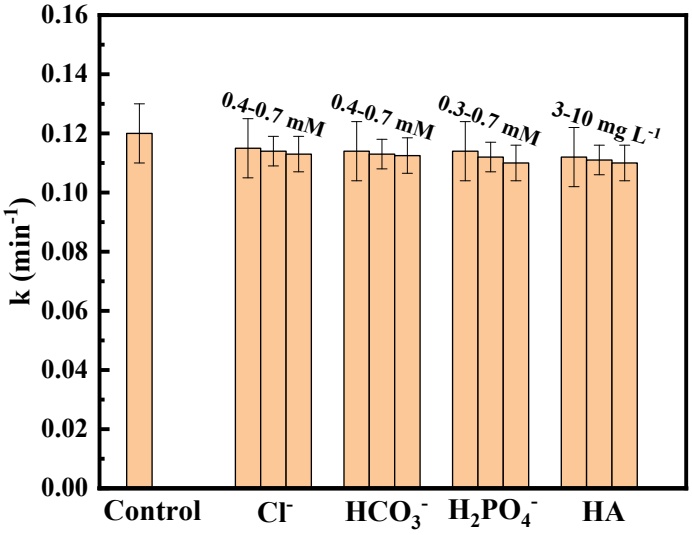

Fig. S7. Reaction rate constants under different experimental conditions.

Table S1 Comparison of PMS activation for TC removal

Catalysts	Catalyst usage	C_{PMS} (g L^{-1})	C_{TC} (mg L^{-1})	Removal	References
CoFe@PPBC	0.1 gL^{-1}	1	50	86.2%	*Sep. Purif. Technol.***2022,** 287, 120533
CoS_x	0.2 gL^{-1}	0.3	30	99%	*Chem. Eng. J.* **2020,** 381, 122768
FONC@PAC	0.5 gL^{-1}	0.45	15	86.9%	*Chem. Eng. J.***2022,** 441, 136061
CoPx@NC	0.1 gL^{-1}	0.3	30	90%	*Sep. Purif. Technol.* **2023,** 322, 124257
Fe_3O_4-NCS_x	0.2 gL^{-1}	0.37	20	97.1%	*Chemosphere* **.2021,** 263, 128011
Co_3O_4/CPANI	0.15 gL^{-1}	0.15	20	92.11%	*J. Clean. Prod.* **2023,** 405, 137023
Co@N-MC	0.04 gL^{-1}	0.2	25	91.27%	*J.Water.Process. Eng.***2023,** 54, 104043
BS900	0.5 gL^{-1}	0.3	40	87.6%	*J. Environ. Chem. Eng.* **2023,** 11(6), 111365
CuCo@GCNs	0.1 gL^{-1}	0.307	20	95.3%	*Chem. Eng. J.* **2022,** 450, 138302
CBB50	0.2 gL^{-1}	0.123	10	90.3%	*Chem. Eng. J.* **2022,** 431, 134054
CW/4Co/2BN QDs	0.2 gL^{-1}	0.3	10	94.8%	*J. Mater. Sci.Technol.* **2024,** 170, 11-24
CuS/g-C_3N_4	0.2 gL^{-1}	0.15	20	97.46%	*Chem. Eng. J.* **2024,**483,149082
BFMO	0.4 gL^{-1}	0.092	50	95.7%	*J. Environ. Chem. Eng.* **2024,** 114338

NiO/SnO_2	0.4 gL^{-1}	0.615	20	90.6%	*Appl. Surf. Sci.* **2022,** 604, 154537
La_2CuO_4	0.2 gL^{-1}	0.615	20	96.05%	*Chemosphere*. **2023,** 332, 138906
$CuFe_2O_4/Bi_2O_3$	0.2 gL^{-1}	0.4	30	95.7%	*Chem. Eng. J.* **2023,**473,145282
FeCo-MOF	0.1 gL^{-1}	0.615	20	91%	*Arab. J. Chem.* **2024,** 17(1),105483
FeS@NBC	0.07 gL^{-1}	0.3	20	87.6%	*J. Environ. Chem. Eng.* **2024,** 12(3), 113027
P-RC-Fe_3O_4	0.1 gL^{-1}	0.3	20	90%	This study

Table S2 The equations for generation of active species

Equations	Serial number
$Fe^{\delta+} + HSO_5^- \rightarrow Fe^{2+} + SO_4^{\cdot-} + OH^-$	(1)
$SO_4^{\cdot-} + H_2O \rightarrow H^+ + SO_4^{2-} + \cdot OH$	(2)
$SO_4^{\cdot-} + OH^- \rightarrow H^+ + SO_4^{2-} + \cdot OH$	(3)
$P^{\delta-} + HSO_5^- \rightarrow PO_4^{3-} + SO4^{\cdot-} + OH^-$	(4)
$SO_4^{\cdot-} + H_2O \rightarrow H^+ + SO_4^{2-} + \cdot OH$	(5)
$HSO_5^- \rightarrow SO_5^{\cdot-} + H^+ + e^-$	(6)
$SO_5^{\cdot-} + SO_5^{\cdot-} \rightarrow S_2O_8^{2-} + {}^1O_2$	(7)
$SO_5^{\cdot-} + SO_5^{\cdot-} \rightarrow 2SO_4^{2-} + {}^1O_2$	(8)
$HSO_5^- + H_2O \rightarrow H_2O_2 + HSO_4^-$	(9)
$H_2O_2 + \cdot OH \rightarrow HO_2\cdot + H_2O$	(10)
$HO_2^{\cdot} \rightarrow O_2^{\cdot-} + H^+$	(11)
$HO_2^{\cdot} \rightarrow O_2^{\cdot-} + H^+ O_2^{\cdot-} + O_2^{\cdot-} + 2H_2O \rightarrow {}^1O_2 + H_2O_2 + 2OH^-$	(12)
$O_2^{\cdot-} + \cdot OH \rightarrow {}^1O_2 + OH^-$	(13)

ROS ($SO_4^{\cdot-}$, ·OH, $O_2^{\cdot-}$,$^1O_2$) + TC → intermediates + CO_2 + H_2O (14)

References

1. Gu, L. L.; Su, Q.; Jiang, W.; Yao, Y.; Pang, Y. J.; Ji, W. J.; Au, C. T., How do the unique Au/α-Fe_2O_3 interfacial structures determine activity in CO oxidation? *Catal. Sci. Technol.* **2018,** *8* (22), 5782-5793.

2. Yin, C.; Li, X.; Dai, Y.; Chen, Z.; Yang, D.; Liu, R.; Zou, W.; Tang, C.; Dong, L., The facet-regulated oxidative dehydrogenation of lactic acid to pyruvic acid on α-Fe_2O_3. *Green Chem.* **2021,** *23* (1), 328-332.